23. Logarithmically growing cells were labeled with TRAN-^{35}S label (ICN) [C. Wittenberg and S. I. Reed, *Cell* **54**, 1061 (1988)], and immunoprecipitations were done essentially as described [M. Hochstrasser and A. Varshavsky, *ibid.* **61**, 697 (1990)] with affinity-purified polyclonal antiserum to Cln2.
24. In vivo [^{32}P]orthophosphate labeling of cells was done essentially as described [J. R. Warner, *Methods Enzymol.* **194**, 423 (1991)]. Logarithmically growing cells were starved for phosphate for 6 to 8 hours, concentrated to one-tenth volume, labeled for 20 min with [^{32}P]orthophosphate (1 mCi/ml), diluted with 4 volumes, and incubated for 1 to 2 hours. Sedimented cells were washed once with ice-cold water, and cell lysis and immunoprecipitation were done as described (*20*) with the following modifications. Lysis buffer contained protease inhibitors [0.4 mM phenylmethylsulfonyl fluoride (PMSF) and 1 μg/ml each of leupeptin, pepstatin A, and aprotinin] and a phosphatase inhibitor mixture (*21*) instead of NaF and EDTA. Before immunoprecipitation with monoclonal antibodies to HA, we denatured proteins by adjusting the extract to 1% SDS and 15 mM dithiothreitol and boiling for 2 min. After centrifugation (15 min at 15,000*g*), extracts were diluted with 9 volumes of immunoprecipitation (IP) buffer (50 mM tris-HCl, pH 7.5, 1% Triton X-100, and 250 mM NaCl, plus protease and phosphatase inhibitors as above). Immune complexes on protein A–Sepharose beads were washed three times with IP buffer, incubated for 30 min on ice in IP buffer containing 200 μg/ml of ribonuclease A, washed once with TBS (100 mM tris-HCl, pH 7.5, and 0.9% NaCl), and boiled in 2× sample buffer.
25. I. A. Wilson *et al.*, *Cell* **37**, 767 (1984).
26. Immune complex protein kinase assays were done essentially as described (*13*). Immune complexes were prepared as described (*20*) with the following modifications. Lysis buffer contained protease inhibitors (0.4 mM PMSF and 1 μg/ml each of leupeptin, pepstatin A, and aprotinin) and a phosphatase inhibitor mixture (*21*) instead of NaF and EDTA. For in vitro phosphorylation of Cln2, histone H1 and unlabeled adenosine triphosphate (ATP) were omitted from the assay.
27. W. J. Boyle *et al.*, *Methods Enzymol.* **201**, 110 (1991).
28. C. Wittenberg, S. L. Richardson, S. I. Reed, *J. Cell Biol.* **105**, 1527 (1987).
29. Site-directed mutagenesis was done on subclones of *CLN2* either with the pALTER system (Promega) or with the polymerase chain reaction. Fragments encompassing the mutated site or sites were subcloned into the TA vector (Invitrogen) and verified by sequencing. To create stable integrants, we subcloned mutated *CLN2* alleles containing wild-type 5′ and 3′ untranslated sequences into pUC18 containing a *HIS2* gene and integrated them at the *his2* locus. To create centromeric vectors containing HA-tagged *CLN2* genes under control of the *GAL1* promoter, we replaced 5′ sequences of a 3′ HA-tagged *CLN2* gene (*22*) with a *GAL1-CLN2* fragment excised from YCpG2 (*2*). Fragments containing *GAL1::CLN2(HA)*$_3$ were then cloned into pRS416 [R. S. Sikorski and P. Hieter, *Genetics* **122**, 19 (1989)].
30. Cell size distributions were analyzed with a Coulter Counter Channelyzer. Mean cell size was determined with a Microsoft Excel–based computer program (S. Lanker and C. Wittenberg, unpublished results).
31. G. F. Sprague Jr., *Methods Enzymol.* **194**, 77 (1991).
32. We constructed *CLN2Δxs*^{4T3S} by deleting the Xho I–Sal I DNA fragment of *CLN2*^{4T3S}, thus creating the same deletion within the cyclin box as in Cln2Δxs (*9*).

33. We thank D. Stuart for the initial *CLN2(HA)*$_3$ construct, M. Guaderrama for expert technical assistance, L. Hengst, C. McGowan, P. Russell, and D. Stuart for helpful discussions and critical reading of the manuscript, and S. Reed for his encouragement at a critical juncture. Supported by U.S. Public Health Services grant GM43487 to C.W. S.L. acknowledges Swiss National Science Foundation and Human Frontier Science Program fellowships. M.H.V. was supported by the Fundación Ramón Areces, Madrid, Spain.

24 October 1995; accepted 1 February 1996

Control of the Gene *optomotor-blind* in *Drosophila* Wing Development by *decapentaplegic* and *wingless*

Stefan Grimm and Gert O. Pflugfelder*

Diffusible factors of several protein families control appendage outgrowth and patterning in both insects and vertebrates. In *Drosophila* wing development, the gene *decapentaplegic* (*dpp*) is expressed along the anteroposterior compartment boundary. Early *wingless* (*wg*) expression is involved in setting up the dorsoventral boundary. Interaction between *dpp*- and *wg*-expressing cells promotes appendage outgrowth. Here, it is shown that *optomotor-blind* (*omb*) expression is required for distal wing development and is controlled by both *dpp* and *wg*. Ectopic *omb* expression can lead to the growth of additional wings. Thus, *omb* is essential for wing development and is controlled by two signaling pathways.

Appendage development in both insects (*1–10*) and vertebrates (*11*) is controlled by conserved diffusible proteins. In *Drosophila*, the wing primordium is divided into compartments by the stable inheritance of selector gene activity (*12*). Appendage development requires the interaction between cells across compartment boundaries. In the wing disc, diffusing HEDGEHOG (HH) protein, synthesized in the posterior compartment under the control of one or more posterior selector genes, directs *dpp* expression in the anterior compartment along the anteroposterior (a-p) boundary (*5, 12*). DPP is required for patterning on both sides of the a-p boundary (*10*). Similarly, the dorsal selector gene *apterous* (*ap*) promotes the synthesis of the diffusible protein FRINGE (*13*). Early *wg* expression is required for establishing the dorsoventral (d-v) boundary (*2, 3*). Interaction between *wg*- and *dpp*-expressing cells promotes the development of the proximodistal (p-d) axis (*4–8*). The presumptive transcription factor OMB plays a critical role in the development of the optic lobes, but it is also essential for the development of the distal wing disc (*14*). We investigated the function of *omb* in wing development and analyzed its relation to *dpp* and *wg*.

Lethal *omb* mutants that survived to the pharate adult stage had severely reduced wings (Fig. 1B). The hypomorphic allele *bifid* [*omb*^{bi}, (*14*)] caused the proximal fusion of all longitudinal veins and led to variable defects at the distal tip of the wing (Fig. 1C). Defects in both regions of the wing blade were enhanced by *omb* null alleles (Fig. 1D) and, dominantly, by mutations in genes required for d-v and a-p patterning

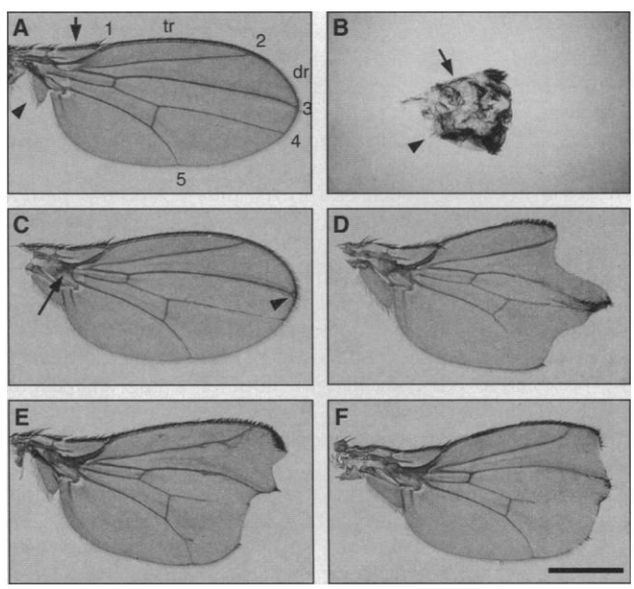

Fig. 1. Wing phenotypes of *omb* alleles and their genetic interactions with d-v and a-p wing patterning genes. (**A**) Pattern elements in the wild-type wing. The longitudinal veins 1 through 5 are numbered where they intersect the wing margin. Triple (tr) and double row (dr) are specializations of the wing margin. The arrow and arrowhead point to anterior (costa) and posterior (alula) elements, respectively. (**B**) Wing from a *l(1)omb*^{3198} (*14*) pharate adult. The proximal elements costa (arrow) and alula (arrowhead) are marked. (**C**) Wing of hypomorphic *omb*^{bi} allele (*14*). All longitudinal veins are fused at the base of the wing (arrow). Distal defects (arrowhead) are variable and temperature-dependent. (**D**) The bifid phenotype is enhanced in combination with all extant lethal *omb* alleles [here, transheterozygote *omb*^{bi}/*l(1)omb*^{3198}]. (**E** and **F**) Dominant enhancement of the omb^{bi} phenotype in *omb*^{bi}/*Y; ap*^{56f}/+ (E) and *omb*^{bi}/*Y*; *dpp*^{d8}/+ (F) individuals. The scale bar in (F) (which applies to all panels) represents 0.5 mm.

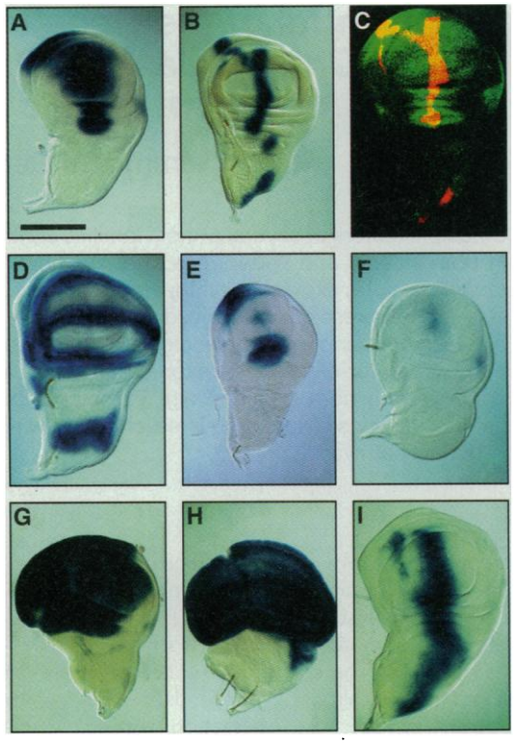

Fig. 2. Control of *omb* expression by *decapentaplegic* and *wingless* in the wing imaginal disc. Wing discs of late third instar larvae are shown. Anterior is to the left and proximal is at the bottom of the panels. For a fate map of wing primordia, see (*28*). All wing discs are at the same magnification [scale bar in (A) is 0.2 mm], except in (G) (1.28-fold lower magnification). Fixation and immunohistochemical staining followed standard procedures (*5, 29*) with polyclonal mouse antibody to OMB (anti-OMB) (*18*) and rabbit anti–β-galactosidase (Cappel) as primary, and fluorescein isothiocyanate–conjugated goat antibody to mouse immunoglobulin G (IgG) and tetramethyl rhodamine isothiocyanate–conjugated goat antibody to rabbit IgG (both Sigma) as secondary antibodies. (**A**) *omb* expression in the omb^{P1} enhancer trap line (*30*). In faintly stained preparations, pouch expression is strongest on the *dpp* stripe [see (B)] and in two stripes flanking the d-v boundary. It is possible that proteins such as CUT which realize the margin fate (*31*) locally repress *omb*. A split *omb* expression domain was also observed when *wg* was ectopically expressed in DPP-positive cells in the notum under the control of the dpp^{blink} enhancer [see (I), (*15*)]. (**B**) *dpp* expression along the a-p compartment boundary in the DPP reporter line BS3.0 (*29*). (**C**) Confocal scanning micrograph of OMB distribution (green) and β-galactosidase expression (red) in BS3.0 (*29*). (**D**) *wg* expression, visualized by a *wg* enhancer trap (*32*), is highly dynamic and develops the pattern shown only in the third instar (*2*). (**E**) *omb* expression is *wg*-dependent. omb^{P1} larvae, homozygous for the temperature-sensitive allele wg^{lL114} were transferred from 16.5°C to the nonpermissive temperature (29°C) for 48 hours before dissection at the end of the third larval instar. During this stage *wg* is no longer required for global wing development (*2*); nonetheless, the wing pouch appears slightly smaller than in the wild type. (**F**) Reduction of *omb* expression in hh^{ts2} larvae. omb^{P1}; hh^{ts2} larvae were held at the nonpermissive temperature (29°C) for 48 hours before dissection in the late third instar. (**G**) Ectopic *omb* expression in omb^{P1}; $Pka^{P113/2}$ mutant wing disc (*17*). (**H**) Expression of *UAS:dpp* under *MS209* Gal4 enhancer trap control (*7*) promotes *omb* transcription to fill the entire wing part of the disc. *MS209* drives gene expression in a broad ring around the wing pouch. (**I**) β-Galactosidase activity in a dpp^{blink}-*Gal4* reporter line (*19*), visualized through *UAS:lacZ*.

such as *ap* and *dpp* (Fig. 1, E and F).

Expression of *omb* in the wing disc develops from a single transcription domain at the distal end of the disc in the second larval instar (*15*) to a more complex pattern in the third larval instar where *omb* is expressed in the wing pouch and in the presumptive hinge region (Fig. 2, A and C). Expression of *omb* does not occur throughout the entire pouch, thus differing from pro-wing genes such as *vestigial* (*vg*) and *scalloped* (*sd*) (*3*). There is no expression in the costa-anlage nor in the proximal part of the prospective posterior margin, both of which are not affected by the loss of *omb* function. In the wing pouch, the expression pattern is mirror symmetrical to both the d-v boundary (visualized by the central stripe of *wg* expression in Fig. 2D) and the a-p boundary (represented by the *dpp* stripe in Fig. 2, B and C). How far WG and DPP can diffuse in the wing disc is unknown, but DPP may act as a long-range morphogen over the entire width of the wing (*10*). Given the genetic interactions with d-v– and a-p–patterning genes and the symmetrical expression of *omb* with regard to both compartment boundaries in the third instar wing disc, it seemed possible that *omb* expression at this stage is controlled by diffusible signals emanating from these boundaries. This hypothesis was tested by analyzing *omb* expression under both loss- and gain-of-function conditions of *wg* and *dpp*.

Inactivation of WG with a temperature-sensitive (ts) allele reduced the expression of *omb* predominantly in the wing pouch (Fig. 2E). Conditional *dpp* alleles are not available. We therefore made use of the *hh* dependence of *dpp* transcription (*5–7, 10*). Upshifting a hh^{ts} mutant (*16*) to the nonpermissive temperature led first to the disappearance of *dpp* and subsequently to the reduction of *omb* expression (Fig. 2F), indicating that DPP rather than HH controls *omb*.

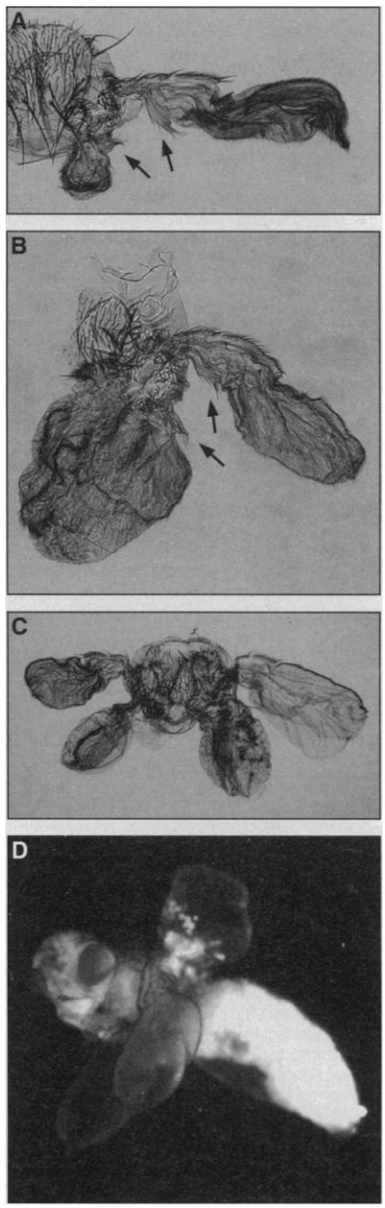

Fig. 3. Ectopic *omb* expression promotes the formation of additional wings. Because of pupal lethality, preparations of pharate adults are shown. (**A**) Formation of an additional wing pair by ectopic expression of *UAS:dpp* under dpp^{blink}-*Gal4* control (see Fig. 2I). The ectopic winglet is located posterodorsally and mirror-symmetrically to the normal wing, as indicated by the opposing alulae. Ten percent of all flies showed outgrowths. (**B** to **D**) Expression of *UAS:omb* (*18*) under dpp^{blink}-*Gal4* control. Anterior elements like costa and triple row are evident in the preparation in (B) but may also be lacking in less fully developed outgrowths. Outgrowths of variable expressivity were observed in 80% of all flies. Location and orientation of the ectopic wings relative to the normal wing pair is as in *UAS:dpp*; dpp^{blink}-*Gal4* animals [compare (C) and (D) with (A)]. The hemithorax preparations in (A) and (B) show the opposing alulae (arrows).

Theodor-Boveri-Institut (Biozentrum), Lehrstuhl für Genetik, Universität Würzburg, Am Hubland, 97074 Würzburg, Germany.

*To whom correspondence should be addressed.

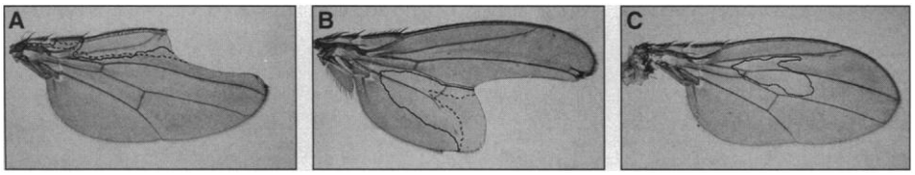

Fig. 4. Mosaic analysis of *omb* requirement in wing development. Mitotic recombinants were obtained by gamma-ray irradiation [10 grays (1 gray = 100 rads) from a ^{137}Cs source] of *y w l(1)omb^{D4} sn^{3} f^{36a}/M(1)o^{Sp}* first instar larvae. The *l(1)omb^{D4}* (*14*) mutant spots in the adult wing blade are marked with the cell autonomous mutations *forked* (*f*) and *yellow* (*y*). The presence of the *Minute* background led to larger clones but otherwise did not affect the results. (**A** and **B**) Severely scalloped wings (not observed in control irradiations) associated with mutant tissue proximal to the lost tissue area. Mutant tissue is outlined by continuous and dashed lines for the dorsal and ventral surface of the wing, respectively. Among 278 wings there was none in which a clone reached an intact distal margin. Seven wings were of the phenotype shown in (A) and (B). (**C**) Internal clone without phenotypic consequences.

The *dpp* dependence of *omb* transcription can also be demonstrated by ectopic *dpp* expression. In the wing disc, reduction of protein kinase A (PKA-C1) activity leads to the ectopic expression of *dpp* in the anterior compartment (*17*). This engenders an anterior expansion of *omb* expression (Fig. 2G). Similarly, ectopic *dpp* expression in a broad ring around the wing pouch leads to a widening of *omb* expression to cover the entire wing domain of the disc (Fig. 2H).

In the wing pouch, *omb* expression is almost completely dependent on both *dpp* and *wg*, whereas in the hinge region *dpp* is sufficient to promote *omb* expression. Pouch and hinge expression are controlled by separate regulatory elements in the *omb* gene (*18*). In the notum part of the disc, the *omb* expression patterns generated by ectopic expression of either *wg* or *dpp* under the control of the *dpp^{blink}* enhancer (see Fig. 2I) suggest that in this ectopic domain, like in the endogenous pouch expression, *omb* is under the joint control of both *dpp* and *wg* (*15*).

Apposition of *dpp*- and *wg*-expressing cells directs proximodistal appendage morphogenesis (*1*, *4*–*6*, *8*, *9*). Transcription of *omb*, too, is dependent on *dpp* and *wg* and is essential for wing development. Therefore, *omb* might mediate a signal that promotes or maintains proximodistal development. Ectopic expression of *omb* in the notum under the control of *dpp^{blink}-Gal4* [(*19*), visualized by *UAS:lacZ* in Fig. 2I] led to the outgrowth of a second wing pair, containing both anterior and posterior margin elements (Fig. 3, B to D). Ectopic wings produced by the expression of *UAS:dpp* under the same *Gal4* control arose in a similar position (Fig. 3A). In the latter case, ectopic wing development probably resulted from coexpression of ectopic *dpp* with endogenous *wg* in its notal expression domain (see Fig. 2D). This also produced ectopic *omb* expression (*15*).

The *omb* expression pattern and the phenotype of *omb* null mutants suggest that *omb* is essential only for the distal wing. We confirmed this by analyzing gamma-ray–induced somatic *omb* wing clones. Clones that reached the margin in the distal half of the wing blade produced severe scalloping (Fig. 4, A and B), whereas internal clones, or clones that reached or crossed the margin proximally, were tolerated without phenotypic consequences (Fig. 4C). Thus, *omb* clones differ from clones in *dpp* or *wg*. *dpp* clones along the a-p boundary are not recovered, whereas *wg* clones lead to marginal notching (*20*), in agreement with the late developmental role of *wg* in margin patterning (*2*). This indicates that *omb* is not involved in all aspects of *dpp* or *wg* function.

The genes *aristaless* (*al*) and *Distalless* (*Dll*) encode homeodomain proteins that are also involved in proximodistal appendage development and appear similarly controlled by *dpp* and *wg* (*4*, *6*, *9*). *Dll* is already expressed in the embryonic appendage anlagen but is only required in larval life to promote limb development beyond the ground state of the surrounding body wall (*21*). *omb*, when expressed ectopically in the notum part of the wing disc, appears to fulfill a role analogous to that of *Dll* in the limbs. In its normal expression domain, however, *omb* is not essential for bulk proliferation. In *omb* null mutants, wing disc tissue is disorganized but reaches nearly wild-type cell numbers in the third larval instar, at which stage apoptosis starts in the *omb* expression domain (*18*). Cell death in the second or third larval instar is common among wing developmental genes [for example, *ap*, *dpp*, *sd*, *vg* (*3*, *22*)], indicating the necessity of genetic control beyond proliferation. The apparent sufficiency of *omb* in the promotion of ectopic wing development and its dispensability for bulk proliferation suggests a redundancy of *omb* function. It is conceivable that an *omb* paralog fulfills related functions in the wing (*18*).

Appendage development in both insects and vertebrates has been discussed theoretically in the framework of the unifiable (*23*) boundary and polar coordinate models (*24*). In the Cartesian boundary model, the intersection of a-p and d-v compartment boundaries specifies the organization of p-d development (*1*, *23*). Both loss- and gain-of-function omb phenotypes point to a role of *omb* in organizing distal wing development.

omb is a member of a gene family, characterized by a novel DNA binding domain (*14*), which in the mouse is expected to comprise up to 20 members (*25*). Several paralogous genes exist in *Drosophila* (*26*). One member of this family, the *Xenopus* homolog of the mouse *Brachyury* gene, acts in mesoderm formation and patterning and is an immediate early gene in response to the transforming growth factor–β cytokine activin A, possibly acting synergistically with a member of the *Wnt* family (*27*). It can therefore be envisioned that OMB-related proteins are part of a conserved signaling module that is used in various developmental contexts.

REFERENCES AND NOTES

1. W. M. Gelbart, *Dev. Suppl.* **107**, 65 (1989).
2. J. P. Couso, M. Bate, A. Martínez-Arias, *Science* **259**, 484 (1993); J. P. Couso, S. A. Bishop, A. Martínez-Arias, *Development* **120**, 621 (1994).
3. J. A. Williams, S. W. Paddock, S. B. Carroll, *Development* **117**, 571 (1993).
4. G. Campbell, T. Weaver, A. Tomlinson, *Cell* **74**, 1113 (1993).
5. K. Basler and G. Struhl, *Nature* **368**, 208 (1994).
6. F. J. Diaz-Benjumea, B. Cohen, S. M. Cohen, *ibid.* **372**, 175 (1994).
7. J. Capdevila and I. Guerrero, *EMBO J.* **13**, 4459 (1994).
8. M. A. Buratovitch and P. J. Bryant, *Dev. Biol.* **168**, 452 (1995); L. I. Held Jr., M. A. Heup, J. M. Sappington, S. D. Peters, *Roux's Arch. Dev. Biol.* **203**, 310 (1994).
9. E. L. Wilder and N. Perrimon, *Development* **121**, 477 (1995).
10. M. Zecca, K. Basler, G. Struhl, *ibid.*, p. 2265.
11. E. Laufer, C. E. Nelson, R. L. Johnson, B. A. Morgan, C. Tabin, *Cell* **79**, 993 (1994); B. A. Parr and A. P. McMahon, *Nature* **374**, 350 (1995); Y. Yang and L. Niswander, *Cell* **80**, 939 (1995).
12. S. S. Blair, *BioEssays* **17**, 299 (1995); F. J. Diaz-Benjumea and S. M. Cohen, *Cell* **75**, 741 (1993); T. Tabata, C. Schwartz, E. Gustavson, Z. Ali, T. B. Kornberg, *Development* **121**, 3359 (1995).
13. K. D. Irvine and E. Wieschaus, *Cell* **79**, 595 (1994); J. Kim, K. D. Irvine, S. B. Carroll, *ibid.* **82**, 795 (1995).
14. G. O. Pflugfelder *et al.*, *Proc. Natl. Acad. Sci. U.S.A.* **89**, 1199 (1992); B. Poeck, A. Hofbauer, G. O. Pflugfelder, *Development* **117**, 1017 (1993); B. Poeck, J. Balles, G. O. Pflugfelder, *Mol. Gen. Genet.* **238**, 325 (1993); G. O. Pflugfelder and M. Heisenberg, *Com. Biochem. Physiol.* **110A**, 185 (1995).
15. S. Grimm and G. O. Pflugfelder, data not shown.
16. C. Ma, Y. Zhou, P. A. Beachy, K. Moses, *Cell* **75**, 927 (1993).
17. D. Pan and G. M. Rubin, *ibid.* **80**, 543 (1995); W. Li, J. T. Ohlmeyer, M. E. Lane, D. Kalderon, *ibid.*, p. 553; J. Jiang and G. Struhl, *ibid.*, p. 563; T. Lepage, S. M. Cohen, F. J. Diaz-Benjumea, S. M. Parkhurst, *Nature* **373**, 711 (1995).
18. J. Balles, S. Grimm, K. Hofmeyer, G. O. Pflugfelder, unpublished results.
19. K. Staehling-Hampton, P. D. Jackson, M. J. Clark, A. H. Brand, F. M. Hoffmann, *Cell Growth Differ.* **5**, 585 (1994).
20. N. E. Baker, *Dev. Biol.* **125**, 96 (1988); L. G. Posakony, L. A. Raftery, W. M. Gelbart, *Mech. Dev.* **33**, 69 (1991).
21. S. M. Cohen and G. Jürgens, *EMBO J.* **8**, 2045 (1989); S. M. Cohen, *Nature* **343**, 173 (1990); B. Cohen, A. A. Simcox, S. M. Cohen, *Development* **117**, 597 (1993).
22. D. Fristrom, *Mol. Gen. Genet.* **103**, 363 (1969); A. A. James and P. J. Bryant, *Dev. Biol.* **85**, 39 (1981); M. Bownes and S. Roberts, *Differentiation* **18**, 89

(1981); P. J. Bryant, *Dev. Biol.* **128**, 386 (1988).
23. H. Meinhardt, *BioEssays* **16**, 627 (1994).
24. P. J. Bryant, *Science* **259**, 471 (1993).
25. R. J. Bollag *et al.*, *Nature Genet.* **7**, 383 (1994).
26. B. Bausenwein, S. Grimm, K. Hofmeyer, G. O. Pflugfelder, unpublished observations; A. Kispert, B. G. Herrmann, M. Leptin, R. Reuter, *Genes Dev.* **8**, 2137 (1994).
27. J. C. Smith, B. M. J. Price, J. B. A. Green, D. Weigel, B. G. Herrmann, *Cell* **67**, 1 (1991); V. Cunliffe and J. C. Smith, *EMBO J.* **13**, 349 (1994).
28. P. J. Bryant, in *The Genetics and Biology of* Drosophila, M. Ashburner and T. R. F. Wright, Eds. (Academic Press, London, 1978), vol. 2c, pp. 229–335.
29. J. D. Masucci, R. J. Miltenberger, F. M. Hoffmann, *Genes Dev.* **4**, 2011 (1990); R. K. Blackman, M. Sanicola, L. A. Raftery, T. Gillevet, W. M. Gelbart, *Development* **111**, 657 (1991).
30. Y. H. Sun *et al.*, *Genetics* **141**, 1075 (1995).
31. J. Williams, S. W. Paddock, K. Vorwerk, S. B. Carroll, *Nature* **368**, 299 (1994).
32. J. A. Kassis, E. Noll, E. P. VanSickle, W. F. Odenwald, N. Perrimon, *Proc. Natl. Acad. Sci. U.S.A.* **89**, 1919 (1992).
33. We thank K. Basler, R. Blackman, S. Cohen, I. Guerrero, F. Jimenez, E. Knust, K. Moses, H. Sun, and the Bowling Green Stock Center for the contribution of stocks; A. Brand and N. Perrimon for providing components of the Gal4/UAS system; S. Wolfrath for fly care; A. Pfränger for irradiation of larvae; A. Hofbauer for immunizations; R. Lierheimer and K. Dücker for hospitality, support at the confocal microscope, and help with the preparation of figures; K. Rein for help in setting up the imaging software; R. Reifegerste for being a help abroad; K. Basler, E. Buchner, and T. Raabe for critiques of the manuscript; and M. Heisenberg for encouragement throughout. Supported by a grant from the Deutsche Forschungsgemeinschaft (G.O.P.).

23 October 1995; accepted 14 February 1996

TECHNICAL COMMENTS

Long-Term Potentiation in the CA1 Hippocampus

Polarized debate continues regarding the locus of the modification responsible for the enhancement of synaptic transmission during long-term potentiation (LTP) in CA1 hippocampus, a widely studied cellular model of learning and memory. Two recent papers (*1*, *2*) have shed light using techniques in which only one or a few axons are stimulated. In this way, transmission may be characterized not only by the mean amplitude of the response (as usual), but also by identifying failures (responses with zero amplitude) and successes of transmission. With LTP, these researchers observe a change in the rate of successes, but no change in the mean amplitude of successes (the "potency"). They argue that such an observation is only compatible with an increased probability of transmitter release, indicating a presynaptic mechanism. They note that postsynaptic changes such as addition of receptors at a transmitting synapse or addition of new synapses (which would occasionally produce simultaneous release at the new and old synapses) would increase potency. However, if LTP is a result of the addition of new synapses [possibly by AMPAfication of pure NMDA synapses (*3*, *4*) or by splitting of existing synapses (*5*)] will the potency necessarily change?

With Monte Carlo simulations of various models, we found that if new synapses recruited during LTP have a smaller response (quantal size, q) than previously existing synapses, the potency need not change (Fig. 1). Intuitively, if a new synapse recruited with LTP has a smaller q, then when the new synapse acts alone, the potency will be decreased; when the old and new synapses act together, the potency will be increased. These effects can cancel each other out, keeping the potency constant. We have considered analytically what requirements are placed on newly transmitting synapses so as to keep the potency constant.

As a simple case, consider one synapse before LTP transmitting with probability of release $p1$, and mean quantal size 1. Let the new synapse added with LTP have a probability of release $p2$ and mean quantal size $q2$. Then,

mean amplitude of transmission before LTP $\equiv$ Mb $= p1$,

mean amplitude of transmission after LTP $\equiv$ Ma $= p1 + p2q2$,

potency before LTP $\equiv$ Pb $=$ Mb/$p1$, and

potency after LTP $\equiv$ Pa $=$ Ma/$\{1 - [(1 - p1)(1 - p2)]\}$.

If we require that Pa = Pb and solve for $q2$, we obtain: $q2 = 1 - p1$.

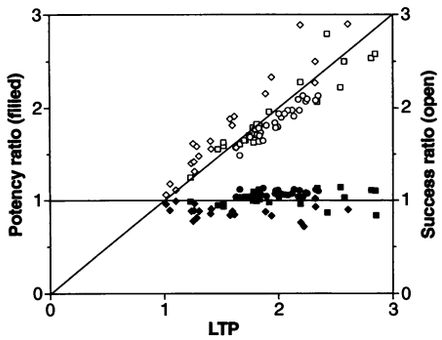

Fig. 1. Changes in potency and success ratio for Monte Carlo simulations of three scenarios in which LTP is produced by adding synapses. For each scenario, 25 experiments each consisting of 250 trials before and after LTP were simulated. Plotted are the ratio of the mean potency before and after LTP (filled symbols) and the ratio of the success probability (fraction of trials with response amplitude >0, open symbols). For each experiment a new set of parameters was chosen randomly from a uniform distribution of specified range (hereafter denoted [min to max]). Circles: one synapse is augmented by a second ($q1 = 1$, $p1$ in [0.15 to 0.45]). Squares: splitting of one synapse ($q = 1$, p in [0.15 to 0.45]) into two ($q1$ and $q2$ in [0.65 to 0.95], $p1$ and $p2$ in [0.15 to 0.45]). Diamonds: addition of synapses under assumption of Poisson statistics (initial population $q1 = 1$, m1 in [0.16 to 0.6], added population $q2$ in [0.55 to 0.85], m2 in [0.16 to 0.6]).

This anlaysis leads us to the puzzling requirement that the response of a new synapse is dependent on the release probability of a previously existing synapse. However, this unsavory demand is not stringent: If we allow for reasonable experimental error in measuring potency, then $q2$ can range considerably (Fig. 2). Similar results are obtained with more general cases (Binomial or Poisson release).

The observation that potency does not change during LTP is not universal, as examples showing changes in potency have been published with minimal stimulation (*3*, *6*) and cell pair recordings (*7*). In our hands, in 6 of 12 experiments with failure rates greater or equal to 50% potency changed more than 20% with pairing-induced LTP (*8*). From the above analysis, we conclude that even in those cases where potency does not change, the underlying mechanism could be addition of new synapses.

A corollary of this result is that manipulations such as paired-pulse facilitation or changes in extracellular calcium may not change potency even if multiple synapses are stimulated, provided these manipulations preferentially act on synapses which have a smaller quantal size. Thus, constant potency during presynaptic perturbations does not necessarily imply stimulation of a

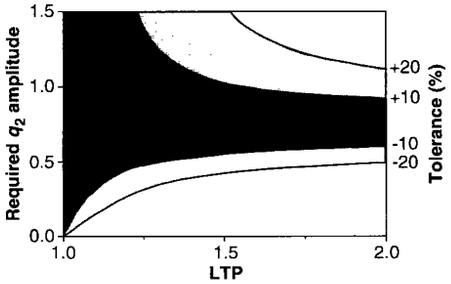

Fig. 2. Requirements on a new synapse to maintain constant potency. A single synapse ($q1 = 1$, $p1 = 0.25$) is augmented by a second synapse to produce LTP. The postsynaptic amplitude $q2$ necessary to maintain potency constant to within a given tolerance and the amount of LTP resulting were computed as functions of $p2$. Tolerances of ±10% and ±20% are shown. Constant potency was more difficult to satisfy with larger LTP (and also with larger initial $p1$, not shown).